OPTICAL-FLOW AND CROSS-CORRELATION ALGORITHMS FOR ANALYZING JET FLOW

Tran The Hung^{1*}, Le Dinh Anh², Nguyen Anh Van¹

¹Le Quy Don Technical University, ²University of Engineering and Technology, Vietnam National University, Hanoi

ARTICLE INFO ABSTRACT

Received: 04/11/2022

Revised: 30/11/2022

Published: 30/11/2022

KEYWORDS

Flow visualization
Optical flow
Particle image velocimetry
Hybrid algorithm
Jet flow

Data processing for obtaining global velocity fields is important in fluid mechanics. This study presents a hybrid algorithm for extracting velocity vectors from particle image velocimetry (PIV) images, which were taken during the experimental process. The hybrid method used both cross-correlation and optical-flow algorithms. Firstly, a crosscorrelation algorithm was used to extract initial velocity from PIV images. The optical-flow algorithm was, then, applied for refined velocity fields with initial estimation by cross-correlation results. The proposed method was applied for recovering velocity vectors from a jet flow. It was shown that the hybrid method shows a similar pattern to the cross-correlation algorithm. Additionally, the resolution was much improved by the proposed algorithm in comparison to cross-correlation results. Both averaged and instantaneous velocity fields were illustrated in this study. The effect of the Lagrange multiplier and interaction number on the results of the hybrid method was investigated. The proposed method shows high ability in extracting velocity fields from PIV images.

227(15): 146 - 154

THUẬT TOÁN XỬ LÝ ẢNH VÀ TƯƠNG QUAN CHÉO TRONG PHÂN TÍCH DÒNG CHẢY VÒI PHUN

Trần Thế Hùng^{1*}, Lê Đình Anh², Nguyễn Anh Văn¹

¹Trường Đại học Kỹ thuật Lê Quý Đôn, ²Trường Đại học Công nghệ, Đại học Quốc gia Hà Nội

THÔNG TIN BÀI BÁO

Ngày nhận bài: 04/11/2022

Ngày hoàn thiện: 30/11/2022

Ngày đăng: 30/11/2022

TỪ KHÓA

Hiển thị dòng chảy

Xử lý ảnh

Phương pháp đo vận tốc ảnh hạt

Thuật toán lai

Dòng chảy vòi phun

TÓM TẮT

Xử lý dữ liệu nhằm thu được trường vận tốc toàn cục rất quan trọng trong cơ học chất lỏng. Nghiên cứu này trình bày thuật toán lai để trích xuất véc tơ vận tốc từ ảnh của phương pháp đo vận tốc ảnh hạt (PIV) thực hiện trong quá trình thực nghiệm. Phương pháp lai sử dụng cả thuật toán tương quan chéo và thuật toán xử lý ảnh. Đầu tiên, thuật toán tương quan chéo được sử dụng để trích xuất vận tốc ban đầu từ ảnh PIV. Sau đó, thuật toán xử lý ảnh được áp dụng cho các trường vận tốc đã được tinh chỉnh với ước lượng ban đầu bằng kết quả tương quan chéo. Phương pháp đề xuất được áp dụng cho phân tích véc tơ vận tốc từ dòng chảy qua vòi phun. Kết quả chỉ ra rằng phương pháp lai thấy hình ảnh tương tự với thuật toán tương quan chéo. Ngoài ra, độ phân giải đã được cải thiện nhiều bởi thuật toán được đề xuất so với kết quả từ phương pháp tương quan chéo. Cả trường vân tốc trung bình và vân tốc tức thời được phân tích trong nghiên cứu này. Ảnh hưởng của hê số Lagrange, số bước lặp tính toán lên kết quả của phương pháp lại được khảo sát. Phương pháp được đề xuất cho thấy hiệu quả cao trong việc trích xuất trường vận tốc từ ảnh PIV.

DOI: https://doi.org/10.34238/tnu-jst.6875

^{*} Corresponding author. Email: tranthehung_k24@lqdtu.edu.vn

1. Introductions

Studying flow is an important topic for researchers in the field of fluid mechanics. Understanding flow behavior around the model allows us to propose a proper control strategy for reducing drag, vibration, and structure facility and increasing the performance of the model. In studying fields of fluid mechanics, two methods, which are numerical simulation and experimental investigation, are widely applied. The numerical method, which is mainly solved the Navier-Stokes equations by a discrete scheme, provides only qualitative results. Different numerical schemes, from RANS [1], mixing of RANS, and Large Eddy Simulation (LES) [2] to LES [3], are capable of practical applications with different levels of accuracy. All relative parameters such as velocity, pressure, temperature, air density, and skin friction around the model can be obtained from the methods. Additionally, the cost of the numerical study is often smaller than experimental methods.

In comparison to numerical study, experimental methods provide only some parameters for each measurement. All device for the measurement is separated or can be connected in some way. The cost for each device is expensive, so each laboratory can provide limitations of the measurements. However, the experimental results provide good validation values for the numerical method. For example, Tran et al. [4], [5] used Reynolds averaged Navier-Stokes equations (RANS) for an extended study of the axisymmetric boattail model. Le et al. [6] used unsteady RANS to study the aerodynamic performance of vertical wind turbines. Additionally, RANS was also applied by Le et al. [7], [8] for the cavitation flow phenomenon. Focusing on the global measurement in experimental methods, data processing on images taken during the experimental process is often applied. For the scalar images such as oil flow on the surface, smoke particle flow, and optical-flow algorithms are used [9]. For discrete distribution of light on the image, such as particle image velocimetry, a cross-correlation algorithm is often applied [10]. However, for the cross-correlation algorithm, an interrogation window is applied for recovering velocity vectors. The size of the windows often ranges from 8×8 pixels to 64×64 pixels, which reduces remarkably the resolution of the velocity fields [11]. The optical-flow algorithm can be applied for PIV images, as investigated by Tran and Chen [12] for the axisymmetric wake model. A comparison of two methods was investigated by Liu et al. [13] for systematic and jet flows. Although the results were much improved, limited cases with the results were revelated.

Another way to recover the high resolution of PIV results is to apply a hybrid method. In this approach, the velocity fields are recovered firstly by cross-correlation algorithms. Then the PIV results are used as initial values for the optical-flow algorithm, which is applied after that. Consequently, the refined velocity vectors can be obtained. The hybrid methods were studied by Yang et al. [14] and Liu et al. [15]. In those studies, similar cross-correlation and optical-flow algorithms were applied. Generally, the hybrid methods provide good results, where relevant numerical parameters were selected [15].

In this study, we proposed a hybrid method for the estimation of flow around the jet model. Difference to the previous study, the optical-flow algorithm was adopted from our previous study, which was used for skin-friction analysis [16]. We show that the hybrid method provides good results in comparison to the optical-flow algorithm. Additionally, by comparison to the cross-correlation algorithm, the resolutions of the flow fields were much improved. In section 2, we present the numerical scheme. The results of the numerical scheme for a jet flow were presented in section 3. Finally, this study concludes in section 4.

2. Methodology

2.1. Cross-correlation algorithm for initial estimations

Generally, the cross-correlation algorithm was widely applied for PIV images in previous studies [11], [17] – [19]. The working principle of PIV is to measure the displacement of small

tracer particles over a short time interval. For this purpose, the luminescent smoke particle was inserted into the wind tunnel section. Then, pair images at different times were captured. For data processing, the cross-correlation algorithm is applied for a small interrogation window in the first and second frames. The position of maximum cross-correlation shows the displacement of the interrogation windows in the second image. Since the time interval between the first and second images was known and displacement of interrogation windows was calculated. Then, instantaneous and averaged flow fields can be recovered. A typical setting of the PIV measurement setup can be shown in Figure 1.

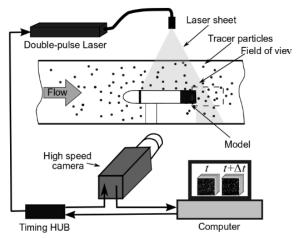


Figure 1. A typical setup for PIV measurement [20]

The cross-correlation formula is indicated as below:

$$R(s) = \int_{W} I_1(X)I_2(X+s)dX \tag{1}$$

where I_1 , and I_2 present the first and second images, X is the coordinate, W is the size of the interrogation window and s is the displacement.

Various factors, such as the diameter of the particles, and the number of averaging images can affect the results of PIV measurement. The methods for evaluation error were presented in previous studies, so it is not shown in the study. Additionally, we focus on the unsteady flow behavior of jet flow with a sufficiently good experimental setup. Consequently, the number of images for averaging flow does not affect to the final results.

As shown in the introduction part, the resolution of the cross-correlation algorithm reduces at least 64 times in comparison to the original image. The low resolution is not suitable for jet flow, where different eddies of turbulent flow occur. Resizing the image using interpolation methods can be applied for increasing the size of the velocity. However, the scale results do not allow to obtain small-scale features of the flow. To overcome this problem, we propose to apply an optical-flow algorithm for scale results from cross-correlation methods. The principle of the optical-flow algorithm is presented in the next section.

2.2. Optical-flow algorithm for velocity refinement

The optical-flow algorithm used in this study was based on the global optical-flow algorithm proposed by Horn and Strunck [21] with additional modifications proposed by Cassian et al. [22], Chen et al. [23], and Tran and Chen [16]. In detail, the equation showing the motion of particles in the measurement image can be written below:

$$\frac{\partial I}{\partial t} + \nabla \Box (I\boldsymbol{u}) = f(x_1, x_2, I) \tag{2}$$

where ∇ is the gradient operator, I is the intensity of the image, u is the velocity vector and f is a function including all outer parameters such as laser thickness and setup of the laser. Practically, f is considered a zero value in the calculation process. Generally, the intensity of the PIV image is discrete, which is not suitable for the optical-flow algorithm. To overcome this problem, a filter is proposed to apply for the whole equation (2), which will then become:

$$\frac{\partial \overline{I}}{\partial t} + \nabla \Box (\overline{u}\overline{I}) + \nabla \Box \tau_s = 0 \tag{3}$$

where \bar{I} and $\bar{u} = \frac{\kappa I}{2\mu} \bar{\tau} - (\nabla p - \rho g) \frac{\kappa^2 I^2}{3\mu}$ are the luminescent intensity, velocity vectors in pixel grid, and τ_s is the sub-grid scalar flux. That parameter is determined by $\tau_s = D_t \nabla I$, where D_t is the turbulent diffusion coefficient.

Equation (3) was solved by the Euler-Lagrange method. In this study, a Lagrange multiplier is applied. Since this study focuses on the location of separation and reattachment flow, we used smoothness term as $J_R = \int_{\Omega} \alpha \|\nabla \overline{u}(x,t)\|^2 dx$. The velocity vectors can be found by minimizing the below equations:

$$J(u) = \int_{\Omega} \left[\frac{\partial \overline{I}}{\partial t} + \overline{u} \Box \nabla \overline{I} + D_t \Delta \overline{I} \right]^2 dx_1 dx_2 + \int_{\Omega} \alpha \left\| \nabla \Box \overline{u}(x, t) \right\|^2 dx_1 dx_2$$

$$\tag{4}$$

Where α is the Lagrange multiplier and is selected before numerical methods. By solving system Eq. (4), the velocity vector can be found. The details of the method for solving Eq. (4) were presented in the previous study by Tran and Chen [16]. The main difference between the current algorithm and previous studies is that the initial velocity is chosen as velocity from PIV results in the current study by comparison to zero value in [16]. Generally, a similar hybrid approach was used by Yang et al. [14] and Liu et al. [15]. In this study, open PIV code was used for cross-correlation results. The methods were built by Thielicke and Stamhuis [24]. The program for the optical-flow algorithm was built by Matlab software.

2.3. Experimental setup for the measurement

To examine the ability of the proposed method in extracting flow fields, we apply the methods for jet flow images, which were conducted by Stanislas et al. [25]. In this study, a high speed was used to capture luminescent smoke particles of free jet flow at a frame rate of 10,000fps. The jet was flown at a nozzle with a diameter of 5 mm with a velocity of 30 m/s. The time between images in a pair was 5 μ m, and a total of 100 image pairs were used for data processing. The size of the image was 512 \times 512 pixels. The data can be downloaded from the challenge website (http://www.pivchallenge.org). Figure 2 shows the two typical images in a pair.





Figure 2. *Image samples in a pair (the time at two images was 5 \mum)*

3. Results for jet flow and discussions

3.1. Flow by different methods

Figure 3 shows the average velocity magnitude by different methods. Here the nozzle of the jet is at the bottom position and the flow from bottom to top. The interrogation window of the method was 8×8 pixels. The velocity was normalized by the free-stream values. The Lagrange parameter for the optical-flow algorithm was chosen at $\alpha = 2000$. As can be seen that the cross-correlation method provides a good pattern of flow. However, the resolution of the flow is reduced from 512×512 pixels to 64×64 pixels. On the opposite side, the optical-flow algorithm can not show the proper velocity fields of the jet flow. It is because of the insufficient smooth intensity on the surface. The results of the hybrid method present a similar pattern to the cross-correlation algorithm. Notably, the resolutions of the flow fields is much improved.

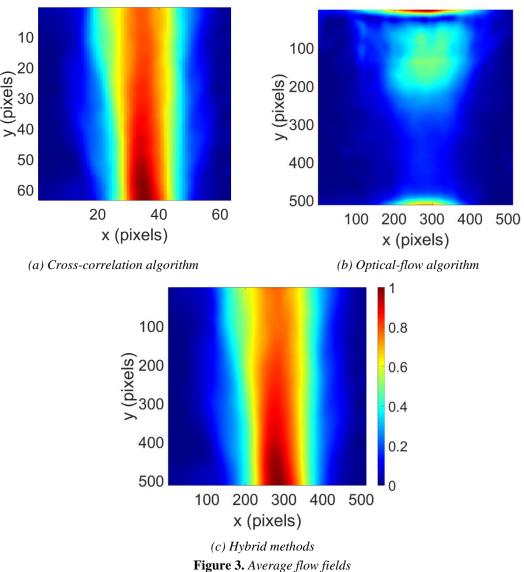


Figure 4 shows the instantaneous velocity magnitude for the pair image 10, which is presented in Figure 2. As can be seen clearly, the hybrid method provides a high resolution of velocity fields. By comparing to the cross-correlation algorithm, some small changes in velocity can be obtained. The ability of the method in extracting flow fields is confirmed.

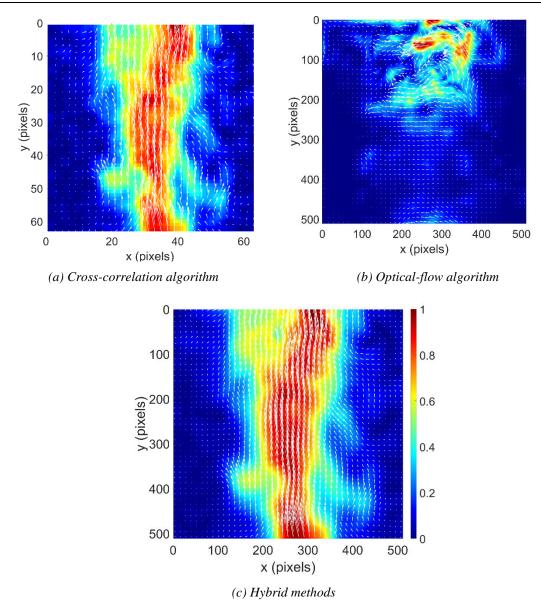


Figure 4. *Instantaneous jet flow for pair image number 10 (image shown in Figure 2)*

3.2. Effect of Lagrange parameters on the results

Figure 5 shows the effect of Lagrange parameters α on the results of velocity magnitude mixing with velocity vectors. Notably, when the Lagrange number is small, the results of the hybrid method shows similar to that of the optical-flow algorithm. Those results are indicated for $\alpha=20$ and $\alpha=200$. As the Lagrange number increases, the results steadily improved. Interestingly, the results become similar for $\alpha\geq2000$. Consequently, it is concluded that the Lagrange number has an effect on the results at low values. In a certain range of Lagrange number, the results become stable. The finding in the hybrid method is similar to the optical-flow algorithm, which was reported before for scale images[26].

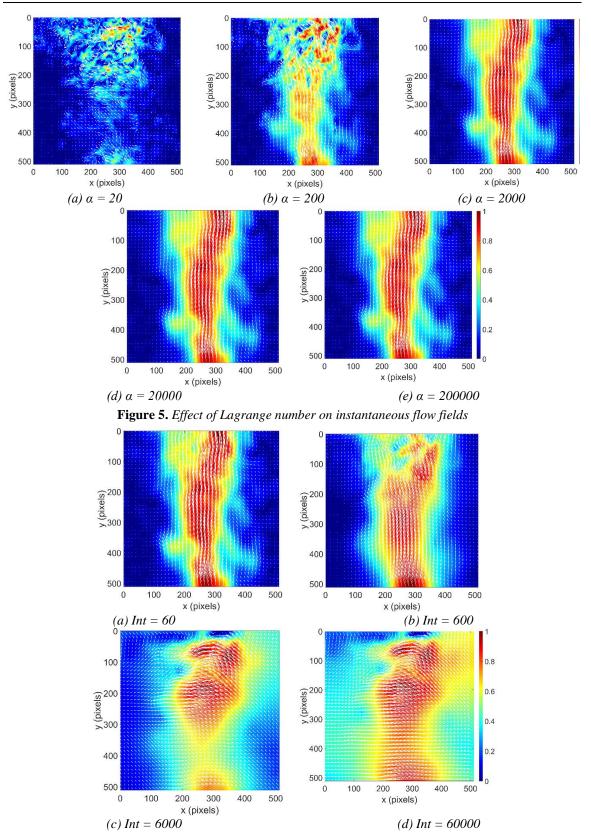


Figure 6. Effect of interaction number on instantaneous flow fields

3.3. Effect of interaction number on the results

Since the interaction was applied for recovering velocity fields in the optical-flow algorithm, the effect of the interaction number on the results was investigated. The investigated results are illustrated in Figure 6. It was shown that when the interaction number is high, the results become smooth and the hybrid method can not capture proper results. An interaction number below 600 is recommended for the optical-flow algorithm in recovering refined velocity fields.

4. Conclusions

A hybrid method for recovering velocity vectors from PIV images was presented in this study. In this measurement, the results of cross-correlation methods were used as the initial estimation of the optical flow algorithm. Then the optical-flow algorithm was applied for refined velocity vectors. The method was then applied to the PIV image of jet flow. The results indicated that the hybrid methods improve the resolution of the velocity vectors. On the opposite, the optical-flow algorithm can not capture properly velocity vectors from the PIV image. The Lagrange multiplier shows little effect on the results when this number is higher than 2000. The interaction number should be selected below 600 in the hybrid method for good results. In further study, the algorithm should be improved and tested for more images to confirm the method.

REFERENCES

- [1] F. R. Menter, "Two-equation eddy-viscosity turbulence models for engineering applications," AIAA J., vol. 32, no. 8, pp. 1598–1605, 1994.
- [2] C. D. Argyropoulos and N. C. Markatos, "Recent advances on the numerical modelling of turbulent flows," *Appl. Math. Model.*, vol. 39, no. 2, pp. 693–732, 2015, doi: 10.1016/j.apm.2014.07.001.
- [3] W. Cheng and R. Samtaney, "A high-resolution code for large eddy simulation of incompressible turbulent boundary layer flows," *Comput. Fluids*, vol. 92, pp. 82–92, 2014, doi: 10.1016/j.compfluid.2013.12.001.
- [4] T. H. Tran, H. Q. Dinh, H. Q. Chu, V. Q. Duong, C. Pham, and V. M. Do, "Effect of boattail angle on near-wake flow and drag of axisymmetric models: a numerical approach," *J. Mech. Sci. Technol.*, vol. 35, no. 2, pp. 563–573, Feb. 2021, doi: 10.1007/s12206-021-0115-1.
- [5] T. H. Tran, D. A. Le, T. M. Nguyen, C. T. Dao, and V. Q. Duong, "Comparison of Numerical and Experimental Methods in Determining Boundary Layer of Axisymmetric Model," in *International Conference on Advanced Mechanical Engineering, Automation and Sustainable Development*, 2022, pp. 297–302.
- [6] A. D. Le, B. M. Duc, T. V. Hoang, and H. T. Tran, "Modified Savonius Wind Turbine for Wind Energy Harvesting in Urban Environments," *J. Fluids Eng.*, vol. 144, no. 8, 2022, Art. no. 081501.
- [7] A. D. Le and T. H. Tran, "Improvement of Mass Transfer Rate Modeling for Prediction of Cavitating Flow," *J. Appl. Fluid Mech.*, vol. 15, no. 2, pp. 551–561, 2022.
- [8] A. D. Le, T. H. Phan, and T. H. Tran, "Assessment of a Homogeneous Model for Simulating a Cavitating Flow in Water Under a Wide Range of Temperatures," *J. Fluids Eng.*, vol. 143, no. 10, 2021, Art. no. 101204, doi: 10.1115/1.4051078.
- [9] T. H. Tran, M. Anyoji, T. Nakashima, K. Shimizu, and A. D. Le, "Experimental Study of the Skin-Friction Topology Around the Ahmed Body in Cross-Wind Conditions," *J. Fluids Eng.*, vol. 144, no. 3, 2022, doi: 10.1115/1.4052418.
- [10]R. J. Adrian and J. Westerweel, *Particle image velocimetry*, vol. 30. Cambridge University Press, 2011.
- [11]T. H. Tran, "The Effect of Boattail Angles on the Near-Wake Structure of Axisymmetric Afterbody Models at Low-Speed Condition," *Int. J. Aerosp. Eng.*, vol. 2020, 2020, doi: 10.1155/2020/7580174.
- [12]T. H. Tran and L. Chen, "Optical-Flow Algorithm for Near-Wake Analysis of Axisymmetric Blunt-Based Body at Low-Speed Conditions," *J. Fluids Eng.*, vol. 142, no. 11, pp. 1–10, 2020, doi: 10.1115/1.4048145.
- [13]T. Liu, A. Merat, M. H. M. Makhmalbaf, C. Fajardo, and P. Merati, "Comparison between optical flow

- and cross-correlation methods for extraction of velocity fields from particle images," *Exp. Fluids*, vol. 56, no. 8, pp. 1–23, 2015.
- [14]Z. Yang and M. Johnson, "Hybrid particle image velocimetry with the combination of cross-correlation and optical flow method," J. Vis., vol. 20, no. 3, pp. 625–638, 2017, doi: 10.1007/s12650-017-0417-7.
- [15]T. Liu, D. M. Salazar, H. Fagehi, H. Ghazwani, J. Montefort, and P. Merati, "Hybrid Optical-Flow-Cross-Correlation Method for Particle Image Velocimetry," *J. Fluids Eng.*, vol. 142, no. 5, pp. 1–7, 2020, doi: 10.1115/1.4045572.
- [16]T. H. Tran and L. Chen, "Wall shear-stress extraction by an optical flow algorithm with a sub-grid formulation," *Acta Mech. Sin. Xuebao*, vol. 37, no. 1, pp. 65–79, 2021, doi: 10.1007/s10409-020-00994-9.
- [17]I. Symposium and P. I. Velocimetry, "Spatio-temporal correlation-variational approach for robust optical flow estimation," *Image*, Rochester, N.Y., September 2007, pp. 11–14.
- [18]J. Venning, D. Lo Jacono, D. Burton, M. Thompson, and J. Sheridan, "The effect of aspect ratio on the wake of the Ahmed body," *Exp. Fluids*, vol. 56, no. 6, 2015, doi: 10.1007/s00348-015-1996-5.
- [19]E. J. Lee and S. J. Lee, "Drag reduction of a heavy vehicle using a modified boat tail with lower inclined air deflector," *J. Vis.*, vol. 20, no. 4, pp. 743–752, 2017, doi: 10.1007/s12650-017-0426-6.
- [20]T. H. Tran, H. Q. Chu, and X. L. Trinh, "Investigation on unsteady behavior of near-wake flow of a blunt-base body by an optical-flow algorithm," *J. Sci. Tech.*, vol. 15, no. 05, pp. 48 59, 2020.
- [21]B. K. Horn and B. G. Schunck, "Determining Optical Flow Berthold," *Tech. Appl. Image Underst.*, vol. 0281, pp. 319–331, 1981.
- [22]C. Cassisa, S. Simoens, V. Prinet, and L. Shao, "Subgrid scale formulation of optical flow for the study of turbulent flow," *Exp. Fluids*, vol. 51, no. 6, pp. 1739–1754, 2011, doi: 10.1007/s00348-011-1180-5.
- [23]X. Chen, P. Zillé, L. Shao, and T. Corpetti, "Optical flow for incompressible turbulence motion estimation," *Exp. Fluids*, vol. 56, no. 1, pp. 1–14, 2015, doi: 10.1007/s00348-014-1874-6.
- [24]W. Thielicke and E. Stamhuis, "PIVlab-towards user-friendly, affordable and accurate digital particle image velocimetry in MATLAB," *J. open Res. Softw.*, vol. 2, no. 1, 2014, doi: 10.5334/jors.bl.
- [25]M. Stanislas, K. Okamoto, C. J. Kähler, J. Westerweel, and F. Scarano, "Main results of the third international PIV challenge," *Exp. Fluids*, vol. 45, no. 1, pp. 27–71, 2008.
- [26]M. Khalid, L. Pénard, and E. Mémin, "Optical flow for image-based river velocity estimation," *Flow Meas. Instrum.*, vol. 65, pp. 110–121, 2019, doi: 10.1016/j. flowmeasinst.2018.11.009